Reinhardt

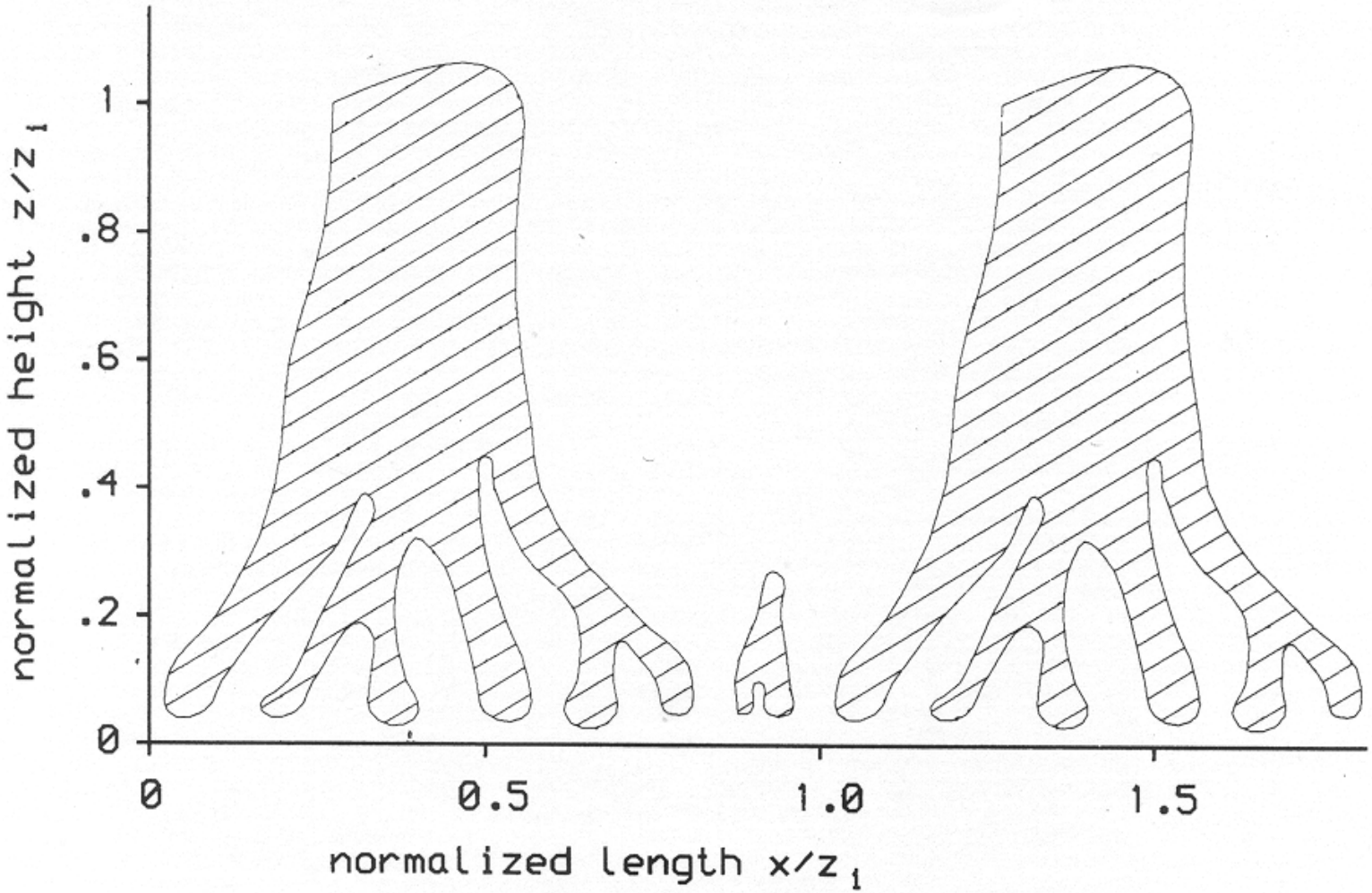

Figure 6. **Conceptual model of thermal field:** Quantitative picture of average x-z-plane.

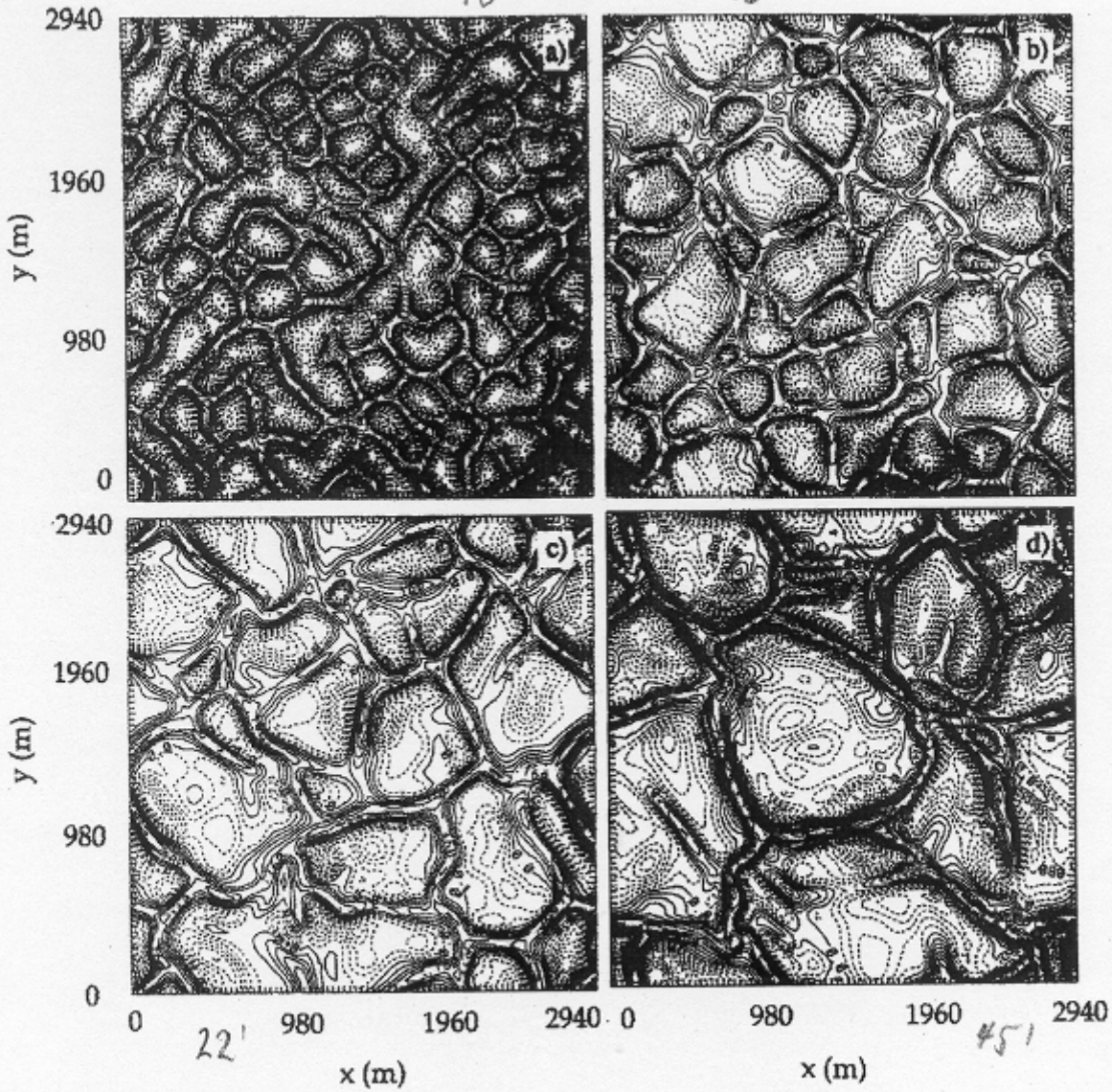

Figure 5. X-Y cross-sections of the vertical velocity at $z = 5.3$ m for: (a) $t = 600$ s, contours from -0.32 to 0.28 with interval 0.04 m s^{-1}; (b) $t = 1000$ s, contours from -0.4 to 0.24 with interval 0.04 m s^{-1}; (c) $t = 1400$ s, contours from -0.36 to 0.28 with interval 0.04 m s^{-1}; and (d) $t = 2800$ s, contours from -0.22 to 0.22 with interval 0.02 m s^{-1}.

Kanak et al

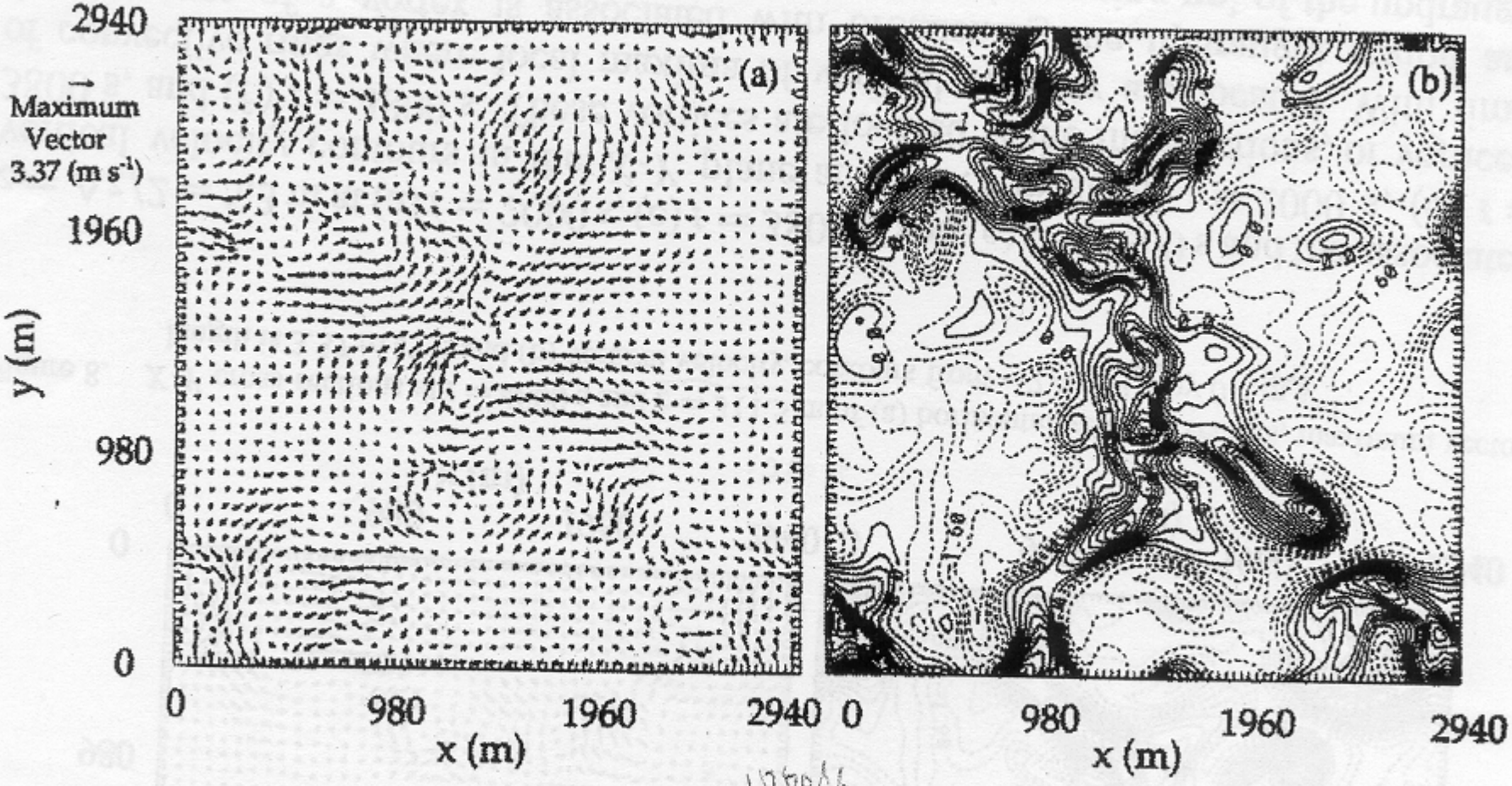

Figure 8. *X-Y* cross-sections at $t = 4800$ s and $z = 311.5$ m of (a) horizontal velocity vectors, maximum vector length is 3.37 m s^{-1}; and (b) vertical velocity, contours from -2.4 to 4.8 by 0.4 m s^{-1}.

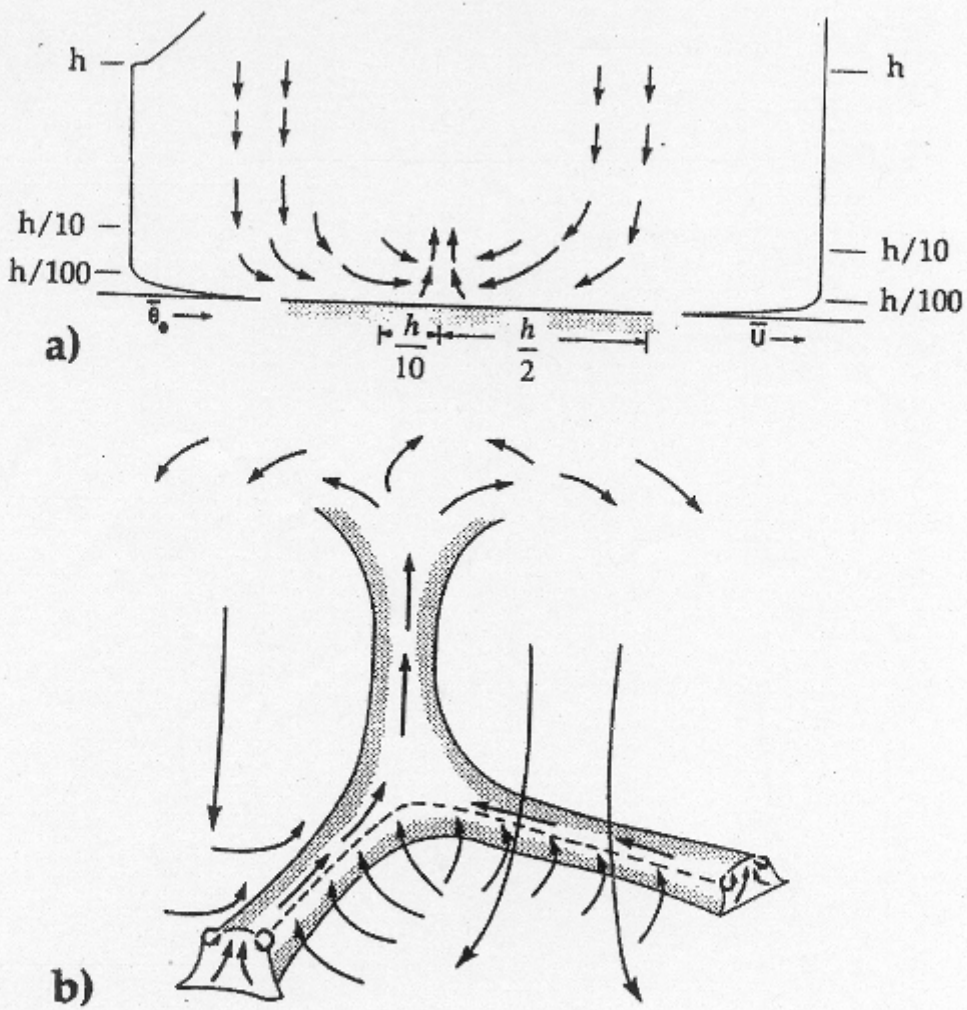

Figure 6. Schematic diagram of the flow patterns for a strongly convective boundary layer. (Note that this has not been drawn to scale.) (a) Vertical cross-section. The horizontal and vertical dimensions of the convection cell are both approximately equal to h, the height of the convective boundary layer. Interactions between downdraughts and updraughts occur over horizontal and vertical dimensions of $\sim h/10$ ($\approx 10|L|$), where L is the Obukhov length, and an updraught wall of height $\sim h/10$ is formed. A layer of strong wind shear and temperature lapse rate occurs between the surface and $\sim h/100$ ($\approx |L|$) $\sim h/100$. A temperature inversion layer caps the boundary layer. Vertical profiles of wind speed $\overline{U}$ and equivalent potential temperature θ_e are shown. (b) A three-dimensional view of the general areas of downdraughts and the updraught walls. At the intersection of walls an updraught column is formed that extends to the top of the boundary layer (based on the measurements of Webb (1977)). (Reproduced from Hess and Spillane (1990)).